

Exchange-field-enhancement of superconducting spin pumping

Kun-Rok Jeon,^{1,2} Chiara Ciccarelli,^{2*} Hidekazu Kurebayashi,³

Lesley F. Cohen,⁴ Xavier Montiel,⁵ Matthias Eschrig,⁵

Sachio Komori,¹ Jason W. A. Robinson,¹ and Mark G. Blamire^{1*}

¹*Department of Materials Science and Metallurgy, University of Cambridge, 27 Charles Babbage Road, Cambridge CB3 0FS, United Kingdom*

²*Cavendish Laboratory, University of Cambridge, Cambridge CB3 0HE, United Kingdom*

³*London Centre for Nanotechnology and Department of Electronic and Electrical Engineering at University of College London, London WC1H 0IH, United Kingdom*

⁴*The Blackett Laboratory, Imperial College London, SW7 2AZ, United Kingdom*

⁵*Department of Physics, Royal Holloway, University of London, Egham Hill, Egham, Surrey TW20 0EX, United Kingdom*

*To whom correspondence should be addressed: cc538@cam.ac.uk, mb52@cam.ac.uk

A recent ferromagnetic resonance study [Jeon *et al.*, Nat. Mat. 17, 499 (2018)] has reported that spin pumping into a singlet superconductor (Nb) can be greatly enhanced over the normal state when the Nb is coupled to a large SOC spin sink such as Pt. This behaviour has been explained in terms of the generation of spin-polarized triplet supercurrents via spin-orbit coupling (SOC) at the Nb/Pt interface, acting in conjunction with a non-locally induced magnetic exchange field. Here we report the effect of adding a ferromagnet (Fe) to act as an internal source of an additional exchange field to the adjacent Pt spin sink. This dramatically enhances the spin pumping efficiency in the superconducting state compared with either Pt

and Fe separately, demonstrating the critical role of the exchange field in generating superconducting spin currents in the Nb.

Spin-triplet Cooper pairs can carry a non-dissipative spin current and are an essential element for the emergent field of superconducting spintronics [1-3]. In the past decade, the generation of spin-polarized triplet pairs within ferromagnets via spin mixing and spin rotation processes at magnetically-inhomogeneous superconductor/ferromagnet (SC/FM) interfaces has been intensively studied [1-4] based on the Josephson effect in SC/FM/SC junctions [5] and the critical temperature T_c modulation in FM/SC/FM and SC/FM/FM' superconducting spin valves [6,7].

Recent theoretical works [8,9] have suggested spin-orbit coupling (SOC) in combination with a magnetic exchange field h_{ex} as an alternative mechanism to generate the spin-polarized triplet supercurrents even at a single magnetically-homogeneous SC/FM interface. Briefly, in the presence of h_{ex} , some of the spin-singlets forming the superconducting condensate of a conventional SC are converted into spin-zero triplets oriented along h_{ex} . If the SOC, originating either from bulk (Dresselhaus-type) or structure (Rashba-type) inversion asymmetry, could have the necessary orthogonality to h_{ex} , the spin-zero triplets rotate to form equal-spin triplets [8,9]. The overall conversion efficiency of spin-singlets to equal-spin triplets is then expected to scale with both the amplitude of h_{ex} and the SOC strength [8,9].

Recent experiments [10-12], have explored the potential role that SOC may play in generating the spin-triplet pair correlations in SC/FM proximity-coupled systems. In particular, our recent ferromagnetic resonance (FMR) study [10] showed that when strong SOC spin sinks (Ta, W, Pt) are added on either side of Nb/Ni₈₀Fe₂₀/Nb samples, spin

pumping [13,14] from the precessing $\text{Ni}_{80}\text{Fe}_{20}$ into the Nb can be substantially larger deep in the superconducting state compared with the normal state. This is the opposite behaviour to what is expected for the spin-singlet superconductivity [15-17], and is attributed to the flow of spin angular momentum through the proximity-induced equal-spin triplet states by SOC, either at the $\text{Ni}_{80}\text{Fe}_{20}/\text{Nb}$ interface [8,9], or possibly at the Nb/Pt interface acting in combination with Landau Fermi-liquid effect [18].

To understand better the mechanisms contributing to enhanced spin pumping in the superconducting state we have conducted a series of experiments on Fe/Pt/Nb/ $\text{Ni}_{80}\text{Fe}_{20}$ /Nb/Pt/Fe structures. Here the ferromagnetic Fe layers serves as an internal source of h_{ex} to the neighbouring Pt spin sink [Fig. 1(a)], creating spontaneous spin splitting, which is known to extend to Pt thicknesses of several nanometres [19]. By comparison with FMR results on Pt/Nb/ $\text{Ni}_{80}\text{Fe}_{20}$ /Nb/Pt control structures without the Fe layers, approximately one order of magnitude enhancement is achieved for certain Pt thicknesses t_{Pt} but this enhancement disappears for large and small t_{Pt} , demonstrating the requirement for *both* SOC and the exchange field in generating substantial superconducting spin currents.

We measured the t_{Pt} dependence of the magnetization M [Fig. 1(b)] and the superconducting transition T_c [Fig. 1(c)] for the two series of samples, with and without the Fe layers. The total M is clearly enhanced by the addition of the Fe layers and it is independent of t_{Pt} , implying that no significant intermixing/interdiffusion occurs at the Pt/Fe interfaces in any of the samples studied. A noteworthy aspect as a function of t_{Pt} is found in the T_c curves: T_c is strongly suppressed by the presence of the Fe layers (about 2 K for $t_{\text{Pt}} = 0$ nm) and the T_c difference becomes smaller as t_{Pt} increases. This proves that the added Fe layers affect the (singlet) superconducting properties of the Nb layer via the

inverse proximity effect, that is, the propagation of Fe-induced exchange (spin-)splitting transmitted through the Pt spacer layer to the Nb/Pt interface [20,21].

To investigate how the Fe-induced h_{ex} influences spin transport, we measured the temperature (T) evolution of the FMR spectra, for instance, the FMR linewidth ($\mu_0\Delta H$) (directly linked to the Gilbert damping α and a measure of the net spin current out of the $\text{Ni}_{80}\text{Fe}_{20}$) and the resonance field (associated with the saturation magnetization $\mu_0 M_s$) [10,13,14]. Note that the zero-frequency line broadening $\mu_0\Delta H_0$ in our system has been found to be less than $|0.5 \text{ mT}|$, which is negligible small for the high frequency regime ($\geq 10 \text{ GHz}$) [10]. Figure 2(a) shows $\mu_0\Delta H$ versus the normalized temperature T/T_c for Pt/Nb/ $\text{Ni}_{80}\text{Fe}_{20}$ /Nb/Pt control structures with different t_{Pt} , taken at a fixed microwave frequency $f=20 \text{ GHz}$. We note that the role of the Pt layers in our system is twofold. One is to proximity-induce equal-spin triplet states in the Nb layers via SOC in combination with hex [8,9]; the other is to provide a dump for spin angular momentum emitted from the middle $\text{Ni}_{80}\text{Fe}_{20}$ layer through the induced triplet states (of the Nb) – a consequence of the very short spin-flip length in Pt [13]. The resulting flow/transfer of spin angular momentum through proximity-induced (equal-spin) triplet states into singlet SCs, namely superconducting spin currents, can then be probed by FMR linewidth broadening or Gilbert damping increase of the middle $\text{Ni}_{80}\text{Fe}_{20}$ [10, 13]. In the normal state ($T/T_c > 1$), $\mu_0\Delta H$ is almost T -independent for all t_{Pt} but increases with increasing t_{Pt} as the Pt becomes a more effective sink for spin current. Upon entering the superconducting state ($T/T_c < 1$), a significant t_{Pt} -dependent evolution of $\mu_0\Delta H(T/T_c)$ takes place: a gradual transition from the narrowing to the broadening of $\mu_0\Delta H$ with the increase of t_{Pt} . This is basically consistent with our previous findings [10], which can be explained by the enhanced spin transfer via induced (equal-spin) triplet states in the Nb via SOC [8,9,18] associated with

the presence of the Pt (5 nm) contrasting with the blocking of spin transport in the samples with small or zero t_{Pt} overwhelmed by the singlet superconductivity

For these Fe-absent control samples, the amplitude of the spin transfer in the superconducting state as measured by $\mu_0\Delta H$ is positively correlated with t_{Pt} . As in the normal state, the effective Pt spin conductance which controls the amount of spin current outflowing [14] from the precessing $\text{Ni}_{80}\text{Fe}_{20}$ diminishes with reducing t_{Pt} ; in addition, the interfacial Nb/Pt SOC which generates triplet spin supercurrents [10,18] should also quickly decrease as t_{Pt} goes to zero.

Figure 2(b) displays $\mu_0\Delta H(T/T_c)$ for Fe/Pt/Nb/ $\text{Ni}_{80}\text{Fe}_{20}$ /Nb/Pt/Fe structures with several t_{Pt} . In the normal state the behaviour is very similar to that of the control samples shown in Fig. 2(a), demonstrating that the addition of the Fe does not enhance the normal spin current. A distinctively different behaviour of $\mu_0\Delta H$ as a function of t_{Pt} appears in the superconducting state when the Fe layers are present – Fig. 2(b) shows that as t_{Pt} increases, the low T suppression of FMR damping for the zero t_{Pt} sample changes to a large damping enhancement at a thinner t_{Pt} with the largest enhancement at the intermediate t_{Pt} of 1.7 nm. This is followed by a slow decrease in damping with $\mu_0\Delta H$ enhancement for the thickest Pt layer (5 nm) similar to the sample without the Fe layers.

To characterize the specific difference in t_{Pt} -dependence between the two series of the samples with [Fig. 2(d)] and without [Fig. 2(c)] the Fe layers, we plotted $\mu_0\Delta H(t_{\text{Pt}})$ for different (constant) T , ranging from 80 to 2 K. For the normal state ($T/T_c > 1$), regardless of the presence of the Fe, $\mu_0\Delta H$ increases in an exponential fashion as a function of t_{Pt} , as expected for diffusive spin transport with the increased Pt spin conductance [13,14]. This normal state behaviour can be quantified using the spin pumping theory [13,14]:

$$\alpha_{sp}(t_{SC}, t_{NM}) = 2 \cdot \left(\frac{g_L \mu_B g_r^{\uparrow\downarrow}}{4\pi M_s t_{FM}} \right) \cdot \left[1 + g_r^{\uparrow\downarrow} \mathcal{R}_{SC} \cdot \left(\frac{1 + g^* \mathcal{R}_{SC} \cdot \tanh\left(\frac{t_{SC}}{l_{sd}^{SC}}\right)}{\tanh\left(\frac{t_{SC}}{l_{sd}^{SC}}\right) + g^* \mathcal{R}_{SC}} \right) \right]^{-1} ;$$

$$g^*(t_{NM}) = g \cdot \left[1 + \frac{g \mathcal{R}_{NM}}{\tanh\left(\frac{t_{NM}}{l_{sd}^{NM}}\right)} \right]^{-1} \quad (1)$$

where g_L is the Landé g-factor, μ_B is the Bohr magneton, and \hbar is Plank's constant divided by 2π . $g_r^{\uparrow\downarrow}$ is the (effective) spin mixing conductance of the Ni₈₀Fe₂₀/Nb interface and g is the (effective) spin transfer conductance of the Nb/Pt interface ($\sim 35 \text{ nm}^{-2}$) [13,22]. $\mathcal{R}_{SC(NM)} \equiv \rho_{SC} l_{sd}^{SC(NM)} e^2 / 2\pi\hbar$ is the spin resistance of the Nb (Pt) layer where ρ_{SC} is the resistivity of the Nb [10], $l_{sd}^{SC(NM)}$ is the spin diffusion length of the Nb (Pt) and e is the electron charge. t_{FM} is the Ni₈₀Fe₂₀ thickness and M_s is its saturation magnetization. Note that the prefactor 2 takes into account the spin pumping through double Ni₈₀Fe₂₀/Nb interfaces [13]. We assumed in Eq. (1) that the addition of a 2.5-nm-thick Fe layers does not much affect the overall spin pumping effect since its spin conductance ($< 3 \text{ nm}^{-2}$) is small relative to other layers [23] – direct evidence for this is the very similar FMR linewidths for the $t_{Pt} = 0$ samples with and without Fe shown in Fig. 2. The similar values of $g_r^{\uparrow\downarrow}$ ($9\text{--}10 \text{ nm}^{-2}$) and l_{sd}^{NM} ($2\text{--}3 \text{ nm}$) are extracted from fitting Eq. (1) to the data of Figs. 2(c) and 2(d), implying comparable spin injection/transport properties of both samples in the normal state. The estimated l_{sd}^{NM} ($2\text{--}3 \text{ nm}$) is consistent with that obtained from spin pumping and inverse spin Hall effect in FM metal/Cu/Pt structures where spin-memory loss at interfaces (*i.e.* interface spin-flip scattering) can be neglected [22,24].

However, for the superconducting state ($T/T_c < 1$), $\mu_0\Delta H(t_{Pt})$ is affected strongly by the presence of the Fe layers. From a comparison of Figs. 2(c) and 2(d), we can see that there is a clear rise in the $\mu_0\Delta H$ enhancement for the $t_{Pt} = 1.7 \text{ nm}$ sample with the Fe

layers. Note also that the superconducting state $\mu_0\Delta H(t_{\text{Pt}})$ deviates from the exponential fashion for both sample sets [Figs. 2(c) and 2(d)] and so it cannot be fitted by Eq. (1). All these results point to a fundamentally different spin transfer mechanism at play deep in the superconducting state when coupled to either Pt or Pt/Fe spin sink.

We show below that this unprecedented spin transfer phenomenon is consistent with a proximity-induced equal-spin triplet pairing generated by SOC [8,9,18] and enhanced by the Fe-induced exchange (spin-)splitting in the Pt.

A quantitative analysis of the effect of the Fe-induced h_{ex} on the superconducting spin transport is available in our present study by comparing the $\mu_0\Delta H$ difference across T_c , defined as $\Delta[\mu_0\Delta H] = \mu_0\Delta H(0.5 \cdot T_c) - \mu_0\Delta H(1.5 \cdot T_c)$, with and without the Fe layers as a function of t_{Pt} [Fig. 3(a)]. In the absence of the Fe layers, $\Delta[\mu_0\Delta H]$ monotonically rises with increasing t_{Pt} and shifts from negative (representing the blocking effect of dominant singlet superconductivity) to positive (indicating enhanced spin transport mediated by triplet pairing). However, when the Fe layers are present, this enhancement becomes more pronounced up to $t_{\text{Pt}} = 1.7$ nm followed a fall to the almost same value for larger thicknesses.

There are several competing effects which lead to this maximum at intermediate thicknesses for the Fe-added samples. Firstly, the interfacial Nb/Pt/(Fe) SOC which appears to be required for triplet spin supercurrent generation [10] should vanish for both sample sets as t_{Pt} goes to zero – in this case there is no triplet pairing and the spin transport via singlet superconducting states should be lower than in the normal state – thus the $t_{\text{Pt}} = 0$ data is similar and negative for both sample sets. Secondly, because the spin conductance of the Fe layers is very small (relative to the Pt layers) [23], the overall Pt/(Fe) spin conductance should be reduced with decreasing t_{Pt} so that for small t_{Pt} even

if triplet pairs are generated, the absorption of superconducting spin currents by the Pt is inactive. Note that the net flow of spin angular momentum through the induced triplet states by SOC (which is what is measured by the FMR spectroscopy) predominantly depends on the effective Pt spin conductance which tends to increase until the Pt thickness becomes comparable to its spin diffusion length [13]. Finally, the exchange field at the Nb/Pt interface is known to increase rapidly with decreasing t_{Pt} in Pt/Fe [19] so that if singlet to triplet pair conversion is indeed further enhanced by the induced h_{ex} , this effect would decay with increasing t_{Pt} , and for large t_{Pt} one would expect the data from the two sample sets to become identical as is the case of for the $t_{Pt} = 5$ nm samples.

Taking these effects together one can see that an intermediate maximum of superconducting spin current might be expected for the samples with Fe as the rapid increase in the induced h_{ex} and hence triplet pair density with decreasing t_{Pt} counteracts the reducing SOC and spin conductance associated with the Pt until the disappearance of the Pt removes the spin sink and SOC from the system at it reverts to singlet behaviour.

One can in principle isolate the contribution of the Fe-induced $h_{ex}(t_{Pt})$ from the other effects of changing Pt thickness by normalizing the t_{Pt} -dependent enhancement of $\Delta[\mu_0\Delta H]$ with the Fe layers (red symbol in Fig. 3) to that without the Fe layers (blue symbol) as follows:

$$\Delta[\mu_0\Delta H(t_{Pt})]_{ex} = \frac{\{\Delta[\mu_0\Delta H(t_{Pt})] - \Delta[\mu_0\Delta H(t_{Pt} = 0)]\}^{w/Fe}}{\{\Delta[\mu_0\Delta H(t_{Pt})] - \Delta[\mu_0\Delta H(t_{Pt} = 0)]\}^{w/o Fe}}. \quad (2)$$

The inset of Fig. 3 shows that $\Delta[\mu_0\Delta H]_{ex}$ goes up rapidly with reducing t_{Pt} , reaching a factor of about 7.5 for 0.8 nm. Essentially, the same behaviour was observed in an analysis based on FMR damping α [Fig. 3(b)], extracted from $\mu_0\Delta H(f)$ [10,13,14] (see Ref. [26] for full details).

We have shown that the spin angular momentum transfer into singlet SCs can be

further enhanced by one order of magnitude when spontaneous spin-splitting in the Pt spin sink is induced by the addition of FM layers. The understanding of SOC generation of superconducting spin currents is still evolving, but the latest theory [18, 27] highlights the need for an induced exchange field in the SOC material. For the Fe-absent samples as reported in our previous paper [10] this is indirectly applied by the spin accumulation at the Pt interface, transmitted by the triplet spin current itself, in combination with Landau Fermi liquid interactions. The key finding of this paper is that superconducting spin pumping can be dramatically enhanced by the influence of the direct exchange field of a coupled ferromagnetic layer on the properties of the Pt layer. This not only provides experimental support for the existing theory of triplet mediated transport [8,9,18], but provides a basis for the development of the comprehensive understanding and optimisation of superconducting spin transport.

This work was supported by EPSRC Programme Grant EP/N017242/1.

References

- [1] J. Linder and J. W. A. Robinson, *Nat. Phys.* **11**, 307 (2015).
- [2] M. Eschrig, *Rep. Prog. Phys.* **78**, 104501 (2015).
- [3] N. O. Birge, *Phil. Trans. R. Soc. A* **376**, 20150150 (2018).
- [4] M. G. Blamire and J. W. A. Robinson, *Journal of Physics: Condensed Matter* **26**, 453201 (2014).
- [5] N. Banerjee, C. B. Smiet, R. G. J. Smits, A. Ozaeta, F. S. Bergeret, M. G. Blamire, and J. W. A. Robinson, *Nat. Comm.* **5**, 4771 (2014).
- [6] S. L. Wang, A. Di Bernardo, N. Banerjee, A. Wells, F. S. Bergeret, M. G. Blamire, and

- J. W. A. Robinson, Phys. Rev. B **89**, 140508(R) (2014).
- [7] A. Srivastava, L. A. B. Olde Olthof, A. Di Bernardo, S. Komori, M. Amado, C. Palomares-Garcia, M. Alidoust, K. Halterman, M. G. Blamire, and J. W. A. Robinson, Phys. Rev. Appl. **8**, 044008 (2017).
- [8] F. S. Bergeret and I. V. Tokatly, Phys. Rev. B **89**, 134517 (2014).
- [9] Sol H. Jacobsen, Jabir A. Ouassou, and J. Linder, Phys. Rev. B **92**, 024510 (2015).
- [10] K.-R. Jeon et al. Nat. Mater. **17**, 499 (2018).
- [11] N. Banerjee, J. A. Ouassou, Y. Zhu, N. A. Stelmashenko, J. Linder, and M. G. Blamire, Phys. Rev. B **97**, 184521 (2018).
- [12] N. Satchell and N. O. Birge, Phys. Rev. B **97**, 214509 (2018).
- [13] Y. Tserkovnyak, A. Brataas, G. E. W. Bauer, and B. I. Halperin, Rev. Mod. Phys. **77**, 1375 (2005).
- [14] K. Ando et al., J. Appl. Phys. **109**, 103913 (2011).
- [15] C. Bell, S. Milikisyants, M. Huber, and J. Aarts, Phys. Rev. Lett. **100**, 047002 (2008).
- [16] J. P. Morten, A. Brataas, G. E. W. Bauer, W. Belzig, and Y. Tserkovnyak, Eur. Phys. Lett. **84**, 57008 (2008).
- [17] T. Wakamura, N. Hasegawa, K. Ohnishi, Y. Niimi, and Y. Otani, Phys. Rev. Lett. **112**, 036602 (2014).
- [18] X. Montiel and M. Eschrig, Phys. Rev. B **98**, 104513 (2018).
- [19] C. Klewe, T. Kuschel, J.-M. Schmalhorst, F. Bertram, O. Kuschel, J. Wollschläger, J. Stempfer, M. Meinert, and G. Reiss, Phys. Rev. B **93**, 214440 (2016).
- [20] M. Vélez, C. Martínez, A. Cebolladab, F. Brionesb, and J. L. Vicentc, J. Magn. Mater. **240**, 580 (2002).
- [21] H. Yamazaki, N. Shannon, and H. Takagi, Phys. Rev. B **81**, 094503 (2010).

- [22] J. C. Rojas-Sánchez et al., *Phys. Rev. Lett.* **112**, 106602 (2014).
- [23] T. Tanaka, H. Kontani, M. Naito, T. Naito, D. S. Hirashima, K. Yamada, and J. Inoue, *Phys. Rev. B* **77**, 165117 (2008).
- [24] M. Caminale, A. Ghosh, S. Auffret, U. Ebels, K. Ollefs, F. Wilhelm, A. Rogalev, and B. E. Bailey, *Phys. Rev. B* **94**, 014414 (2016).
- [25] A. I. Gubin, K. S. Il'in, S. A. Vitusevich, M. Siegel, and N. Klein, *Phys. Rev. B* **72**, 064503 (2005).
- [26] See Supplemental Material at [URL will be inserted by publisher] for a detailed analysis of MW frequency dependence of FMR spectra for the samples with and without the Fe layers at low temperatures, effect of the Fe thickness on overall FMR spectra of Fe/Pt/Nb/Ni₈₀Fe₂₀/Nb/Pt/Fe samples, and experimental details.
- [27] In our theoretical work [18], the equilibrium spin currents have been calculated to demonstrate the long-range triplet correlations, but they are not to be equated with the pumped non-equilibrium spin currents. Although quantitative details and mathematical descriptions need to be fully set out, it is evident that with the presence of equilibrium equal-spin triplet pairs in the entire structure, a new channel is opened for spin currents to be transmitted through a singlet SC to Pt spin sink.

Figures

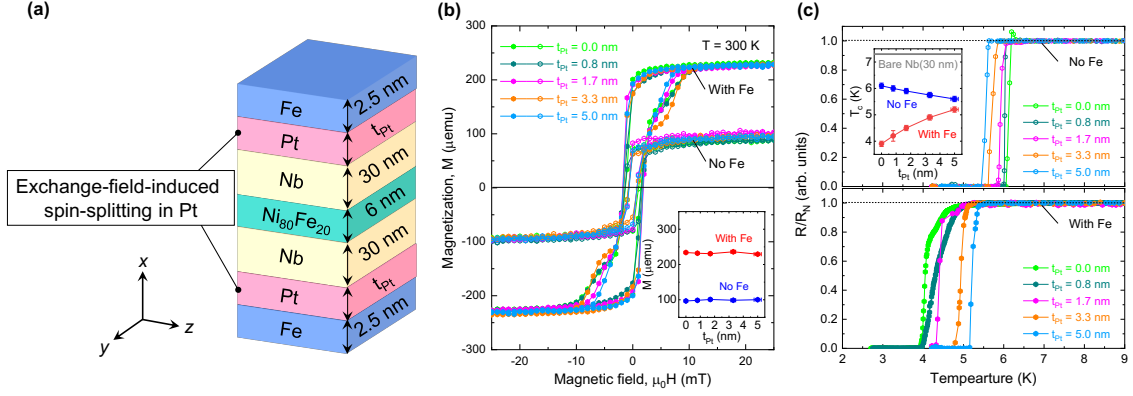


FIG. 1. Structural, magnetic properties and induced exchange field in Fe/Pt/Nb/Ni₈₀Fe₂₀/Nb/Pt/Fe structures. (a) Schematic of the Fe(2.5 nm)/Pt(t_{Pt})/Nb(30 nm)/Ni₈₀Fe₂₀(6 nm)/Nb(30 nm)/Pt(t_{Pt})/Fe(2.5 nm) samples with different Pt thicknesses t_{Pt} and a Cartesian coordinate system used in present study. (b) In-plane magnetization M curves of the two series of samples with and without the Fe layers. The inset summarizes the t_{Pt} dependence of total M of the samples. (c) Normalized resistance R/R_N vs. temperature T plots for the two series of samples with and without the Fe layers. The inset summarizes the t_{Pt} dependence of the superconducting transition temperature T_c of the samples; for comparison, T_c of a bare Nb(30 nm) film is also shown. Error bars denote standard deviation of multiple measurements.

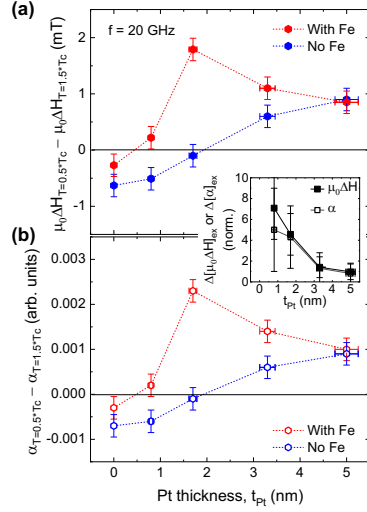


FIG. 2. Characterization of exchange field effect on spin transport in the superconducting state. (a) Normalized temperature T/T_c dependence of the FMR linewidth $\mu_0\Delta H$ (top) and the resonance magnetic field $\mu_0 H_{res}$ (bottom) for Pt(t_{Pt})/Nb(30 nm)/Ni₈₀Fe₂₀(6 nm)/Nb(30 nm)/Pt(t_{Pt}) control samples with various Pt thicknesses t_{Pt} . The dashed lines in the top panel are given as guides to the eyes. The inset shows the calculated superconducting energy gap $2\Delta(t_{Pt})$ from the measured $T_c(t_{Pt})$ [Fig. 1(c)] as a function of T/T_c . This provides information about how much the added Fe layers further suppress $2\Delta(t_{Pt})$ via inverse proximity effect [20,21] in addition to the conventional (singlet) superconducting proximity effect. (b) Data equivalent to (a) but for Fe(2.5 nm)/Pt(t_{Pt})/Nb(30 nm)/Ni₈₀Fe₂₀(6 nm)/Nb(30 nm)/Pt(t_{Pt})/Fe(2.5 nm) samples. (c) FMR linewidth $\mu_0\Delta H$ as a function of t_{Pt} of the Pt/Nb/Ni₈₀Fe₂₀/Nb/Pt control samples at various T . The solid lines are fits to estimate the effective values of spin mixing conductance at the Ni₈₀Fe₂₀/Nb interface and spin diffusion length of the Pt using the spin pumping model [13,14]. The inset shows data and fits for the normal state. (d) Data equivalent to (c) now for the Fe/Pt/Nb/Ni₈₀Fe₂₀/Nb/Pt/Fe samples. Error bars denote standard deviation of multiple measurements.

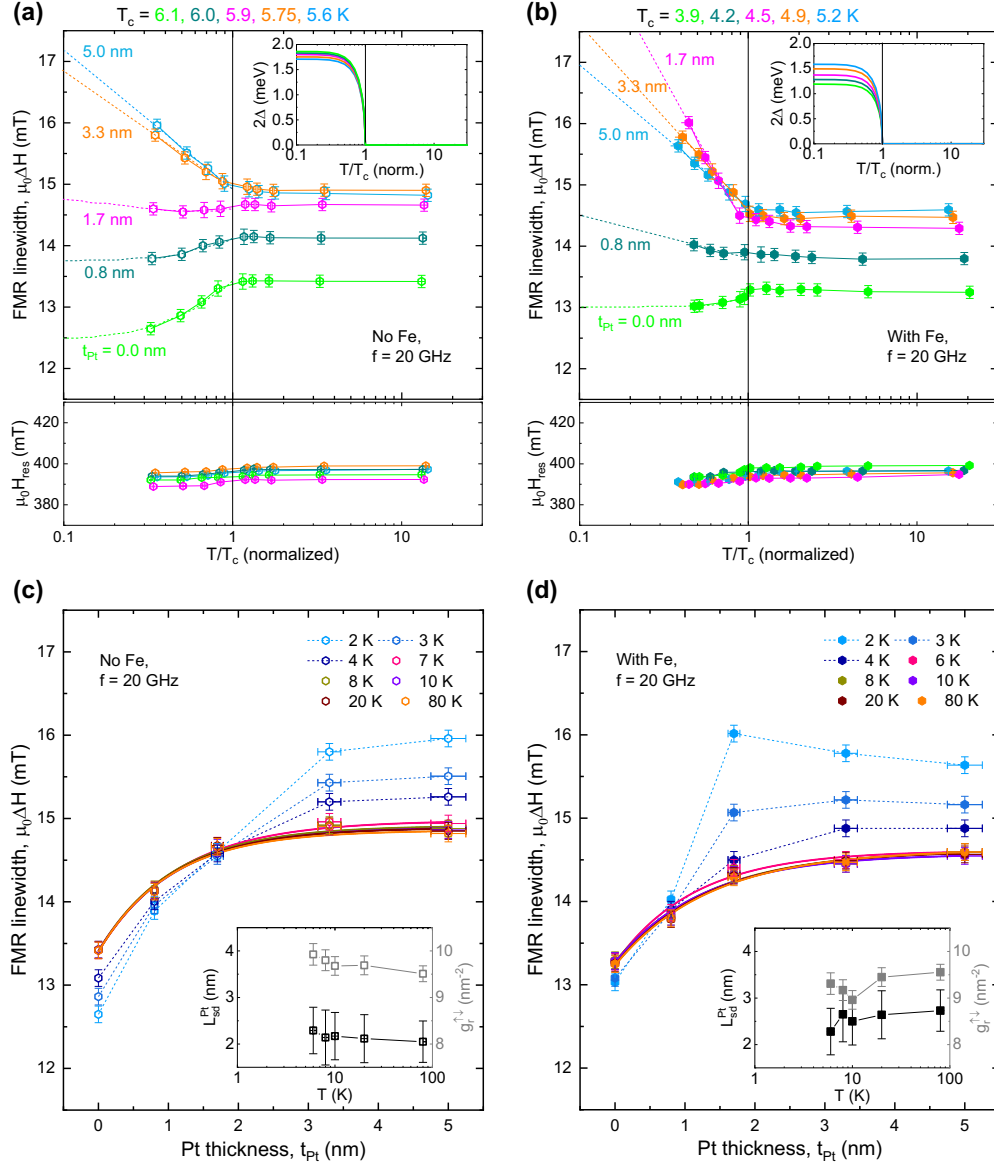


FIG. 3. Exchange-field-enhanced spin transport in the superconducting state. (a) Pt thickness t_{Pt} dependence of the FMR linewidth $\mu_0\Delta H$ difference across T_c , defined as $\Delta[\mu_0\Delta H] = \mu_0\Delta H(0.5 \cdot T_c) - \mu_0\Delta H(1.5 \cdot T_c)$, with and without the Fe layers. (b) Data equivalent to (a) for the Gilbert damping α [13,14]. The inset shows the estimated contribution of the Fe-induced exchange field h_{ex} to the spin transport, denoted as $\Delta[\mu_0\Delta H]_{ex}$ or $\Delta[\alpha]_{ex}$, as a function of t_{Pt} . Error bars denote standard deviation of multiple measurements.

